Published in IET Microwaves, Antennas & Propagation
Received on 13th August 2008
Revised on 21st February 2009
doi: 10.1049/iet-map.2008.0274

ISSN 1751-8725

Coupled structural–electromagnetic–thermal modelling and analysis of active phased array antennas

C.S. Wang[1] *B.Y. Duan*[1,2] *F.S. Zhang*[2] *M.B. Zhu*[1]

[1]*School of Electromechanical Engineering, Xidian University, Xi'an 710071, People's Republic of China*
[2]*National Key Laboratory of Antenna and Microwave Technology, Xidian University, Xi'an 710071, People's Republic of China*
E-mail: congsiwang@gmail.com

Abstract: The electromagnetic performance of an active phased array antenna (APAA) is obviously degraded because of structural distortion caused by thermal power consumption and exterior load. The coupled structural–electromagnetic–thermal (SET) model of APAA is developed on the analysis of the phase difference of radiating elements in the aperture field caused by structural displacement including load–displacement and thermal distortion of structure. Based on the cascade coupled finite element analysis of antenna structure, thermal distortion and other structural distortions are obtained. The coupled SET model is verified by analysing the degradation of the electromagnetic performances of a planar hexagonal APAA operating under different temperature distributions and structural constraints.

1 Introduction

Phased array technology is a developing one, which widely affects radar than most other technologies such as single-impulse technology and impulse Doppler technology. Active phased array antenna (APAA) technology can satisfy the requirement for high performance and high survival ability, and is also a way of decreasing the cost of radar, whose electromagnetic (EM) performance and process period have a direct influence on the performance and cost of radar [1–5]. Generally, APAA contains two parts: one is the radiation part including the antenna array and reflector; the other is the feed part involving the transmit/receive module (TRM), the beam control module, power and RF rotary joint etc. The supporting body of the whole APAA consists of outer and inner frames, which are subject to exterior loads such as wind load, vibration load and so on. For example, structural distortion is generated when APAA operates under an airborne, missile-borne, vehicle-borne and space borne environment. APAA structure is the carrier and boundary condition of electromagnetic signal transmission, with its displacement field directly influencing the amplitude and phase distribution of the EM field. Subsequently, the antenna's shape and size, and the flatness of the array plane have a direct influence on the EM performances of APAA such as sidelobe level (SLL), beam pointing and gain [6–8]. The exothermic modular of APAA mainly covers thousands of TRMs assembled in the antenna array and the high-density packaging power with a thermal value at the kW level, which result in antenna structural distortion and a temperature shift in the devices [9]. Consequently, the heat-induced structural distortion and TRM's performance degradation should also be taken into account. That is to say, the temperature field of the array plane also plays an important role in the distribution of the structural displacement field. Therefore there does exist a close interactive relationship among the structural, EM and thermal designs, a problem called a coupled structural–electromagnetic–thermal (SET) problem.

Because the performance of a phased array radar system is directly influenced by the degradation of EM performances of APAA, some researchers explored the different influencing factors of antenna EM performances. Wang [10] investigated the influence of the random error of a radiating element on the performance of a phased array antenna based on the probability method. But this assumed that structural error met a pregiven distribution and did

not analyse the practical structural error through the finite element analysis of antenna structure. Zaghloul *et al.* [11] discussed the influence of array distortion errors on EM performances. However, this only regarded the root-mean-square (RMS) value of the flatness of an array plane as the evaluation standard and did not consider the different effects of each radiating element with different errors on the antenna performance. Li and Gao [12] analysed radiating element failure using the statistical approach. Jiang *et al.* [13] stated the influence of RMS error of the element phase on antenna performance. Ruze [14] showed the result generated by the lateral and longitudinal displacements of space feed. Mollah [15] exhibited the influence of the variation of the filling factor of the EM bandgap on the phase properties of array antenna. Li and Gao [12], Jiang *et al.* [13], Ruze [14] and Mollah [15] explored the influencing factors of the far radiation field of APAA, but did not examine the effect of structural distortion such as radiating element displacement. Adelman and Padula [16] implemented an integrated thermal–structural–electromagnetic optimisation design by a cascade coupled method. Liu and Hollaway [17] realised a coupled structural–electromagnetic design of reflector antenna by a multidisciplinary model with two optimisation objects. However, Adelman and Padula [16] and Liu and Hollaway [17] did not analyse whether the quantitative relationship exists between structural parameters and EM performances. Joshi *et al.* [18] showed how to analyse a coupled RF–thermal–structural–RF. But only application in the high-intensity proton linac was studied. Ye [19] set a coupled three-dimensional (3-D) flow and thermal model of APAA. Nakagawa *et al.* [20] developed a thermal design scheme of APAA. Ye [19] and Nakagawa *et al.* [20] were limited to research on cooling technology without describing the influence of temperature of an array plane on antenna EM performances.

An antenna is a mechatronic system whose structural design should conform to the requirement for structural intensity and stiffness and whose thermal design should reduce the temperature effect. However, the most important purpose of antenna design is that EM performances should meet the limitation. Therefore it is a beneficial way of achieving the optimal synthesis design of APAA by studying the coupled SET problems and investigating the relationship among structure factor, temperature distribution and EM performance based on the finite element analysis. Thus, the authors studied the coupling relationship between the structural displacement field and the EM field of reflector antennas, and presented a coupled structural–electromagnetic model that directly described antenna EM performance (the gain reduction coefficient) as the function of structural design variables [21]. But it is solely applicable to parabolic reflector antennas. With radar antennas developing for high-frequency band and high gain, low SLL and high performance, and ultra-width band and high precision [22–25], the coupled SET problems of APAA become increasingly serious. Therefore based on the previous studies of authors, the paper investigates the relationship among structural displacement field, temperature field and EM field, and discusses the coupled SET solution method of APAA.

2 Coupled SET modelling of APAA

APAA errors mainly include feed errors and structural ones. The changed position and height difference of radiating elements with structural error both degrade the amplitude and phase of excitation current and the phase distribution of the aperture field of APAA. Structural errors also generate feed error, for instance the change in feed resistance and inconsistent polarisation direction. The structural displacement error of APAA mainly comes from two aspects: one is the systemic structural distortion resulting from environmental loads such as thermal power consumption, solar radiation and vibration etc, and the other is the random structural error generated in an antenna's manufacturing, processing and assembling. All these errors degrade the EM performances of APAA, for example SLL upgrade, inaccurate beam pointing and gain loss.

2.1 Analysis of the structural displacement field

The structural displacement field of APAA is defined as the new space structural shape of an antenna, which is formed by the deviation of structural nodes from the original position when the antenna structure is distorted under exterior loads. The structural displacement field varies with time and space. And the deviation vector of a node is the very displacement vector of the node in the displacement field. The definition is given mainly from the perspective of engineering application, which differs from the physical concept of the EM field. That is to say, the antenna structural displacement field has a boundary and without what is called strong and weak physical fields. Also, the structural displacement field consists only of different displacement quantities of structural nodes. The structural displacement field does not distribute in any space region, but only in its defined region that is the antenna structure system. The structural displacement field, unlike the EM field and the temperature field, has no direct force on the objects in the field, but as a representation of energy it transmits the action of one object to the other object by the stress field.

The distribution of the structural displacement field of APAA is determined by the equation

$$\boldsymbol{K}\boldsymbol{\delta} = \boldsymbol{F} \tag{1}$$

where $\boldsymbol{K}$ is the stiffness matrix with the displacement vector $\boldsymbol{\delta}(\beta_1, \beta_2, \ldots, \beta_R)$ of structure, which is a function of

doi: 10.1049/iet-map.2008.0274

structural design variables β_i ($i = 1, 2, \ldots, R$). The structural design variables include variables of size, shape, topology and type. $\boldsymbol{F}$ is the vector of the node loads comprising weight, static wind load and thermal load.

When APAA operates under dynamic loads, the new analysis equation of the structural displacement field of APAA is given as

$$\boldsymbol{M}\ddot{\boldsymbol{\delta}} + \boldsymbol{C}\dot{\boldsymbol{\delta}} + \boldsymbol{K}\boldsymbol{\delta} = \boldsymbol{F} \tag{2}$$

where $\boldsymbol{M}$ is the mass matrix of structure, $\boldsymbol{C}$ is the damping matrix, $\boldsymbol{F}$ is the dynamic load vector including transient wind load, vibration and impact force and $\ddot{\boldsymbol{\delta}}$ and $\dot{\boldsymbol{\delta}}$ are the acceleration and speed vector of nodes, respectively.

2.2 Analysis of the temperature field

Because of the heat produced by TRMs, the heat flux density of the array plane can amount to 2–30 W/cm^2. Structural temperature and structural distortion are increased by the highly concentrated radiating elements. The aim of thermal design and analysis of APAA is to reduce structural temperature, thus making the devices operate under a suitable temperature range and all TRMs possibly work under the same temperature. Owing to the requirement of a phase shifter for temperature, the highest and lowest temperatures of an array plane should differ by less than 10°C, or else the performance of the phase shifter would be degraded dramatically.

To analyse the relationship between temperature field and structural displacement field of APAA, firstly an accurate thermal model of APAA should be set up with the temperature analysis to determine the temperature distribution. Secondly, the obtained structural temperature is taken as the temperature load of the model of APAA. Then the coupled thermal–structural analysis of APAA is made to determine the thermal distortion of APAA structure by using the available thermal strain of structure. Therefore the fluid characteristic of the convective heat transfer is described generally on the basis of computational fluid dynamics (CFD). The calculation method for the temperature field produced by air or liquid flow and heat is adopted to analyse the structural temperature of APAA simultaneously.

2.3 Coupled SET model of APAA

According to the influencing relationship between the position deviation of radiating elements caused by the structural distortion and EM performance of planar hexagonal APAA and rectangular APAA explored in Appendices 8 and 9, a coupled SET model of APAA is developed based on the finite element analysis of structure as follows

$$\begin{aligned} E(\theta, \phi) = \sum_{m=0}^{M-1}\sum_{n=0}^{N-1} E'_{mn}(\theta, \phi) I'_{mn} \\ \times \exp\left\{ \mathrm{j}k\left[\left(md_x + \sum_{i=0}^{m} \Delta x_{ij}(\boldsymbol{\delta}, \boldsymbol{T}) \right) f_x(\theta, \phi) \right.\right. \\ + \left(nd_y + \sum_{j=0}^{n} \Delta y_{ij}(\boldsymbol{\delta}, \boldsymbol{T}) \right) f_y(\theta, \phi) \\ \left.\left. + \Delta z_{ij}(\boldsymbol{\delta}, \boldsymbol{T}) f_z(\theta) \right] + \mathrm{j}S_{mn}(\boldsymbol{T}) \right\} \end{aligned} \tag{3}$$

where $E(\theta, \phi)$ is the pattern function, $\boldsymbol{T}$ is the structure temperature, $\boldsymbol{\delta}(\beta_1, \beta_2, \ldots, \beta_R)$ is the structural displacement, β_i ($i = 1, 2, \ldots, R$) are the structural design variables, $f_x(\theta, \phi), f_y(\theta, \phi)$ and $f_z(\theta)$ are a function of element position and direction determined by the array arrangement form like hexagonal APAA and rectangular APAA, $\Delta x_{ij}(\boldsymbol{\delta}, \boldsymbol{T}), \Delta y_{ij}(\boldsymbol{\delta}, \boldsymbol{T})$ and $\Delta z_{ij}(\boldsymbol{\delta}, \boldsymbol{T})$ are the deviation values of the element position determined by $\boldsymbol{T}$ and $\boldsymbol{\delta}$, $S_{mn}(\boldsymbol{T})$ is the array phase difference controlled by the phase shifter affected by $\boldsymbol{T}$, and d_x and d_y are the intervals of radiating elements.

I'_{mn} is the amplitude of excitation current considering the mutual coupling effects of an array element expressed as

$$I'_{mn} = I_{mn} + \sum_{p=0}^{M-1}\sum_{q=0}^{N-1} S_{mn,pq} I_{pq} \tag{4}$$

where $S_{mn,pq}$ is the scattering coefficient of an array element.

$E'_{mn}(\theta, \phi)$ is the pattern function of radiating elements in an antenna array given as

$$\begin{aligned} E'_{mn}(\theta, \phi) = E_{\mathrm{e}}(\theta, \phi) \sum_{p=0}^{M-1}\sum_{q=0}^{N-1} S'_{mn,pq} \exp\{\mathrm{j}k[(p-m)d_x f_x(\theta, \phi) \\ + (q-n)d_y f_y(\theta, \phi)]\} \end{aligned} \tag{5}$$

where $E_{\mathrm{e}}(\theta, \phi)$ is the ideal pattern function of the radiating element. The scattering coefficient $S'_{mn,pq}$ is obtained as

$$S'_{mn,pq} = \begin{cases} 1 + S_{mn,pq}, & p = m, \quad q = n \\ S_{mn,pq}, & p \neq m \quad \text{and/or} \quad q \neq n \end{cases}$$

The coupled SET model of APAA indicates that SLL degrades with antenna structural distortion, and is independent of the amplitude of element excitation. In developing the coupled SET model, it is found that the phase difference may be compensated by the available structural distortion (the position deviation of the radiating element) to improve EM performances. Moreover, the deduction of the coupled model is applicable to other

APAA systems with different arrangements such as octagonal and circular APAA. Then according to the coupled SET model of APAA, the distribution function of directive gain is obtained as

$$G(\theta_0, \phi_0) = 10\log\frac{4\pi E^2(\theta_0, \phi_0)}{\int_0^{2\pi}\int_0^{\pi} E^2(\theta, \phi)\sin\theta\,\mathrm{d}\theta\,\mathrm{d}\phi} \quad (6)$$

where (θ_0, ϕ_0) are the elevation and azimuth for APAA gain pattern.

Supposing $E'(\theta, \phi) = E(\theta, \phi)/E_{\max}$, the gain G in the maximum radiation direction is derived as

$$G = 10\log\frac{4\pi}{\int_0^{2\pi}\int_0^{\pi} [E'(\theta, \phi)]^2\sin\theta\,\mathrm{d}\theta\,\mathrm{d}\phi} \quad (7)$$

3 Solution to the coupled SET model of APAA

Based on the characteristic of the coupled SET model, the cascade coupled algorithm is adopted to solve and analyse the coupled SET model. Meanwhile, finite element analysis is used to accurately calculate the temperature and structural displacement of APAA. Here the structural displacement includes the load–displacement and thermal distortion of structure. The flow chart of the solution to the coupled SET model is shown in Fig. 1.

The basic coupling solution seen from Fig. 1 is (i) to derive the temperature and thermal strain of structure induced by the thermal power consumption of APAA based on thermal analysis, (ii) to obtain the structural displacement caused by thermal load and exterior load based on finite element analysis, (iii) to determine the array distortion of APAA, (iv) to investigate the influence of the temperature of TRM on the amplitude and phase of excitation current, (v) to analyse the radiation electrical field of radiating elements [26] and (vi) to calculate the EM performances of APAA based on the coupled SET analysis.

3.1 Structural solution principle

The different solution methods of structure are used in the different loads. For example, for static loads such as static wind load, solar radiation and self weight, the appropriate boundary condition should be given according to the constraint characteristics of structure and environment. Then the total stiffness matrix of APAA is obtained. The solution to the structural displacement is obtained using (1). Although the exterior load is dynamic load such as dynamic wind load and vibration and impact force, the equivalent power spectral function of dynamic load varying with time should be determined. The dynamic response of APAA structure is obtained using (2). The full constraint of structure should be made to avoid an incorrect analytical result.

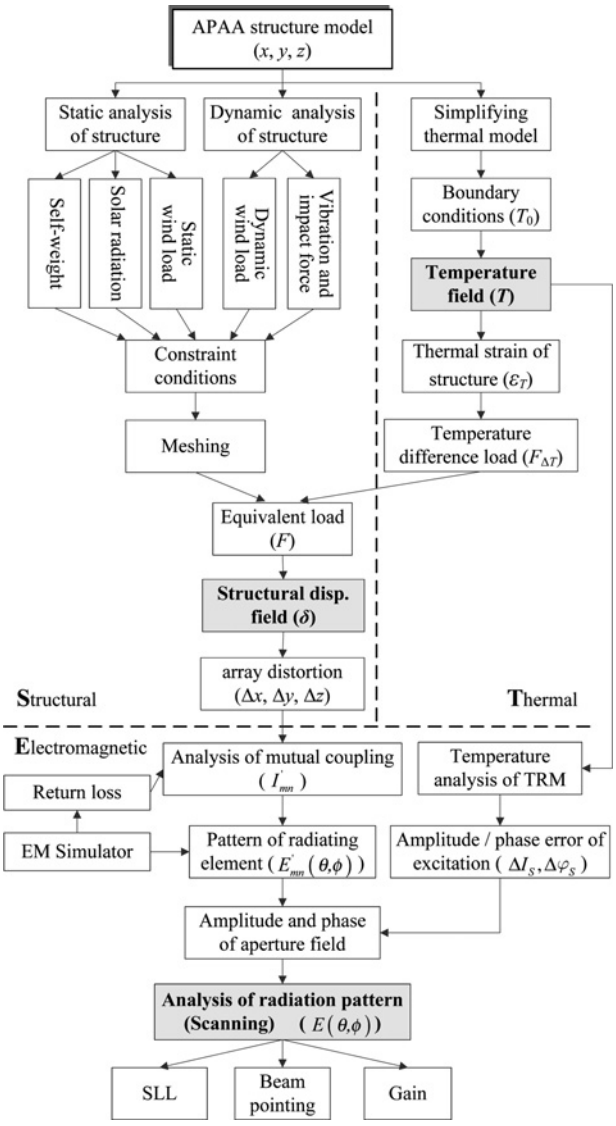

Figure 1 *Flow chart of solution to coupled SET model of APAA*

3.2 Thermal solution principle

The accurate thermal model of APAA should be set up before thermal analysis to obtain structure temperature, which involves material parameters of structure, cooling manner, reference temperature of the environment, thermal power of TRM, size and physical parameters of radiator, shape and size of the wind tunnel and so on [27]. The result of temperature analysis has a great difference because of the different thermal parameters of APAA. Due to several parts involved, for instance thousands of TRMs, the symmetry of APAA structure may as well be adopted to simplify the thermal model, reduce the difficulty of modelling and increase the efficiency of modelling.

It is assumed that the influence of thermal distortion of structure on thermal parameters is not considered. Then, the thermal strain of structure caused by the structure

doi: 10.1049/iet-map.2008.0274

temperature difference of APAA is shown as

$$\begin{aligned}\boldsymbol{\varepsilon}_{\Delta T} &= [(\varepsilon_x \quad \varepsilon_y \quad \varepsilon_z \quad \gamma_{yz} \quad \gamma_{xz} \quad \gamma_{xy})_i^{\mathrm{T}}] \\ &= \alpha(\boldsymbol{T} - \boldsymbol{T}_0)[1 \quad 1 \quad 1 \quad 0 \quad 0 \quad 0]^{\mathrm{T}} \\ &= \alpha\Delta\boldsymbol{T}[1 \quad 1 \quad 1 \quad 0 \quad 0 \quad 0]^{\mathrm{T}} \end{aligned} \tag{8}$$

Hence the temperature difference load intensity of APAA is derived as

$$\boldsymbol{\sigma}_{\Delta T} = \boldsymbol{D}\boldsymbol{\varepsilon}_{\Delta T} = \frac{E\alpha\Delta\boldsymbol{T}}{1-2u}[1 \quad 1 \quad 1 \quad 0 \quad 0 \quad 0]^{\mathrm{T}} \tag{9}$$

Therefore the solution equation of structure temperature difference load of APAA is obtained as

$$\boldsymbol{F}_{\Delta T} = \left[\int_{\mathrm{v}} \boldsymbol{B}^{\mathrm{T}}\boldsymbol{\sigma}_{\Delta T}\mathrm{d}v\right] \tag{10}$$

where $\boldsymbol{T}_0$ is the initial reference temperature of APAA, $\boldsymbol{T}$ is the calculating temperature, $\boldsymbol{\varepsilon}_{\Delta T}$ is the structure strain caused by the temperature, $\Delta\boldsymbol{T}$ is the temperature difference of structure, α is the coefficient of thermal dilatation of structure, E is the elastic modulus of structure, u is Poisson's ratio of structure, $\boldsymbol{D}$ is the 3-D elasticity matrix of structure, $\boldsymbol{B}$ is the strain matrix of structure, $\boldsymbol{\sigma}_{\Delta T}$ is the temperature difference load intensity and $\boldsymbol{F}_{\Delta T}$ is the equivalent load induced by the temperature difference.

3.3 EM solution principle

After the determination of structure displacement, the position deviation of radiating elements is derived. Then to obtain the pattern of radiating elements, the analysis of the mutual coupling of radiating elements is made by using the impedance method or some EM simulator such as IE3D, AWR and HFSS [28]. Therefore the amplitude and phase error of the aperture field of APAA caused by structural distortion is obtained. After the implementation of thermal analysis of APAA, the temperature of TRM is also found. Then, the amplitude and phase error of the excitation current is determined using the fitted temperature shift curve of TRM, whereafter, the far electrical field distribution is analysed that is also the radiation pattern. The scanning pattern of APAA is also investigated simultaneously. By using the antenna pattern, the EM performances of APAA such as SLL, beam pointing and gain are determined based on the coupled SET analysis results above.

4 Results and discussion

A coupled SET analysis of a planar hexagonal APAA seen in Fig. 2 is done as follows. The mutual coupling between radiating elements and the influence of temperature distribution of structure on TRM and excitation current are not considered here. The operation frequency is 26 GHz. The radiating element is a half-wave dipole. The 14 wind tunnels are set in the antenna frame with rectangular cross

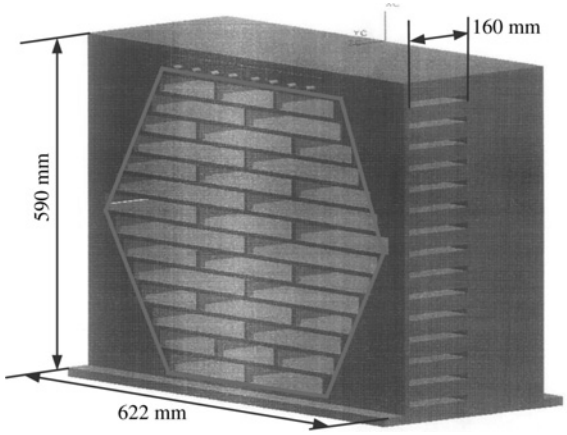

Figure 2 *Planar hexagonal APAA structure frame*

section. The size of the wind tunnel is 622 × 160 × 30 mm. The 182 TRMs are assembled in the array plane. The TRM has a tiled multilayer structure. The arrangement of TRMs in the half part below APAA is shown in Fig. 3. The thickness and interval of the heatsinks are both 4 mm. The size of the simplified TRM model is 130 × 22 × 20 mm. The horizontal and vertical intervals of the radiating element are 22 and 30 mm, respectively. The radiating element is simplified as a cylinder with a diameter of 5 mm in the thermal model. By computer simulation technology (CST) simulation, the lowest return loss ($-S_{11}$) of radiating elements is 22.4371 dB. Because only half of the array plane is modelled, the symmetrical constraint is made on the upper half part of the array plane. The three-degree-of-freedom constraints of the four nodes in the back and 16 nodes at the bottom of the antenna frame are made (as shown in Fig. 4*a*).

To ensure the conformability of the structural and thermal model of APAA and the correct transmission of the thermal load, the preprocess module GAMBIT in CFD software Fluent is used to set up the thermal model. The temperature field of APAA calculated in Fluent is exerted on the structure model established in FE software ANSYS as thermal load. The size of the mesh of the antenna frame

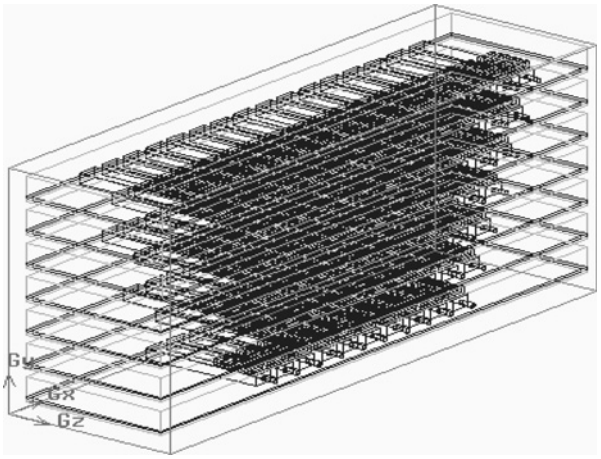

Figure 3 *Arrangement diagram of TRM*

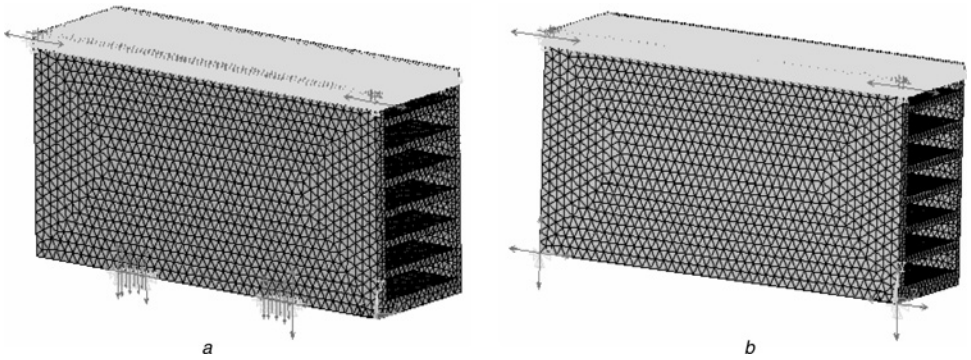

Figure 4 *Finite-element model and constraint of an antenna structure*

a Original constraint
b New constraint

is 10 mm. The size of the mesh of TRM is 8 mm. The total number of mesh elements of the fluid and solid model is 15 65 795. The components and heat conductivity of APAA are listed in Table 1. The other physical parameters are shown in Table 2. The heat conductivity between the outer frame and the outer surface of the array plane is 7 W/m^2K. The first-order upwind difference scheme is used in the discrete representation of momentum and energy equations. The format of the Spalart–Allamaras model is adopted in the turbulence equation. The implicit separation solution in a thermal solver and the SIMPLE algorithm in a series of pressure correction algorithms are used. The pressure and speed correction coefficients in the SIMPLE algorithm are 0.3 and 0.7, respectively.

The first operation condition: APAA is heat soaked at 50 and 90°C, respectively, with the original constraint shown in Fig. 4*a*. The second operation condition: APAA operates at two temperature gradients of 40–50 and 40–70°C, respectively, with the original constraint. The third operation condition: APAA is heat soaked at 60°C with original and new constraints. The latter is with four nodes in backup structure shown in Fig. 4*b*. The gain patterns of APAA under three different operation conditions with $\phi = 0$ and 90° are shown in Figs. 5, 6 and 7, respectively. The maximum gain and gain loss of APAA are listed in Table 3.

The simulation results in the figures and Table 3 indicate the following: (i) the directive gain loss is increased and SLL rises with increase in the temperature of the heat-soaked array plane. The higher the temperature of the array plane, the more serious the degradation of the EM performances. (ii) The directive gain loss of APAA at a temperature gradient of 40–70°C is greater than that at a temperature gradient of 40–50°C. The directive gain loss and the rise of SLL are directly proportional to the temperature gradient. That is to say, the greater the temperature gradient, the more serious the degradation of the EM performances. (iii) The directive gain loss of APAA with the new constraint is less than one with the original constraint. With the new constraint condition, the degradation of SLL is more serious. Therefore the constraint format of structure has a direct effect on EM performances.

What can be concluded by comparing the coupled SET simulation results of APAA under three different conditions are the following: the same temperature of APAA structure has different influences on the antenna gain pattern of the two azimuth planes. The same structural distortion has an

Table 1 Components and heat conductivity of APAA

Components	Material	Heat conductivity W/(m K)	Components	Material	Heat conductivity W/(m K)
antenna frame	hard aluminium alloy	202	fluid	stable air	0.32
radiating element	hard aluminium alloy	202	chip	COMP	20
TRM	hard aluminium alloy	202	delivery tube	AL	214
substrate	LTCC	1	insulating layer	poor conductor	/

IET Microw. Antennas Propag., 2010, Vol. 4, Iss. 2, pp. 247–257
doi: 10.1049/iet-map.2008.0274

Table 2 Physical parameters of APAA

Hard aluminium alloy				Environmental temperature	Absolute reference temperature
Density	Elastic modulus	Coefficient of thermal dilatation	Poisson's ratio		
2.84E3 kg/m^3	70 GPa	2.3E-5/°C	0.33	25°C	0°C
TRM					
Input power	Out power	Insertion loss	Bit	VSWR	Thermal power
40 W	400 W	2 dB	6	$\leq$1.5	6 W

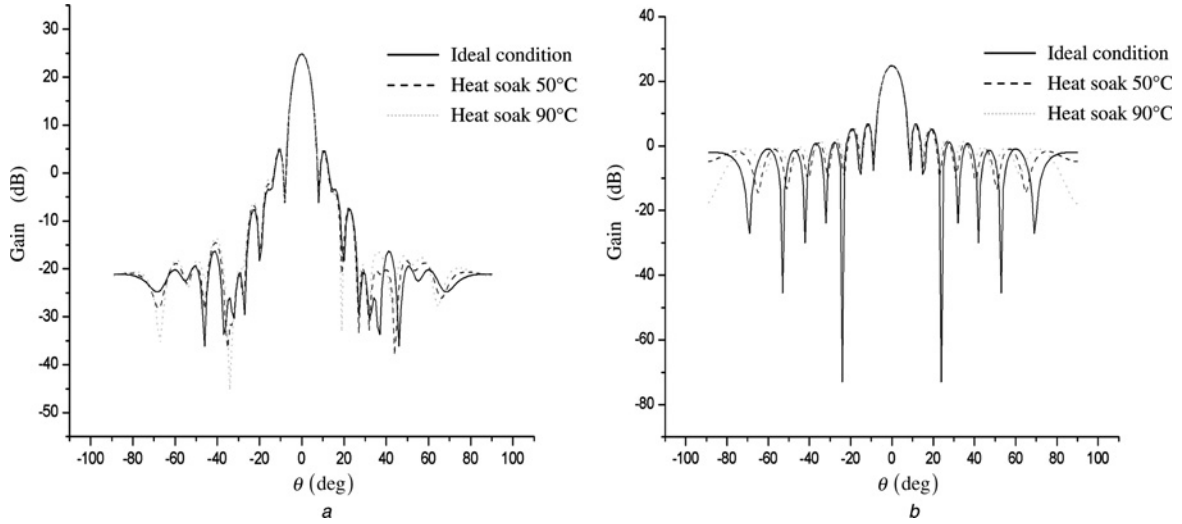

Figure 5 *Antenna gain pattern under first operation condition*
a $\phi = 0^\circ$
b $\phi = 90^\circ$

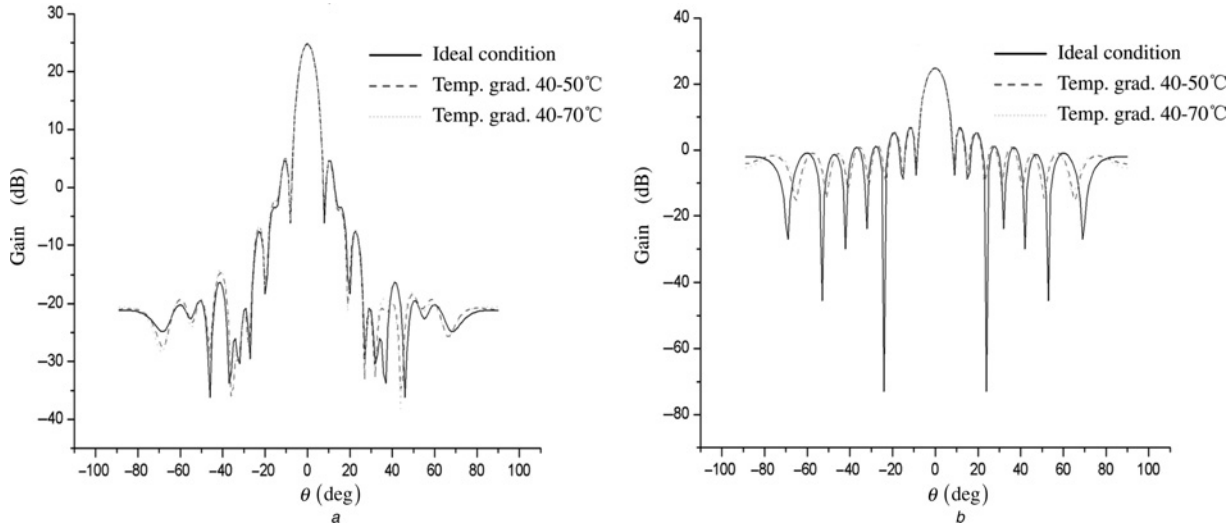

Figure 6 *Antenna gain pattern under second operation condition*
a $\phi = 0^\circ$
b $\phi = 90^\circ$

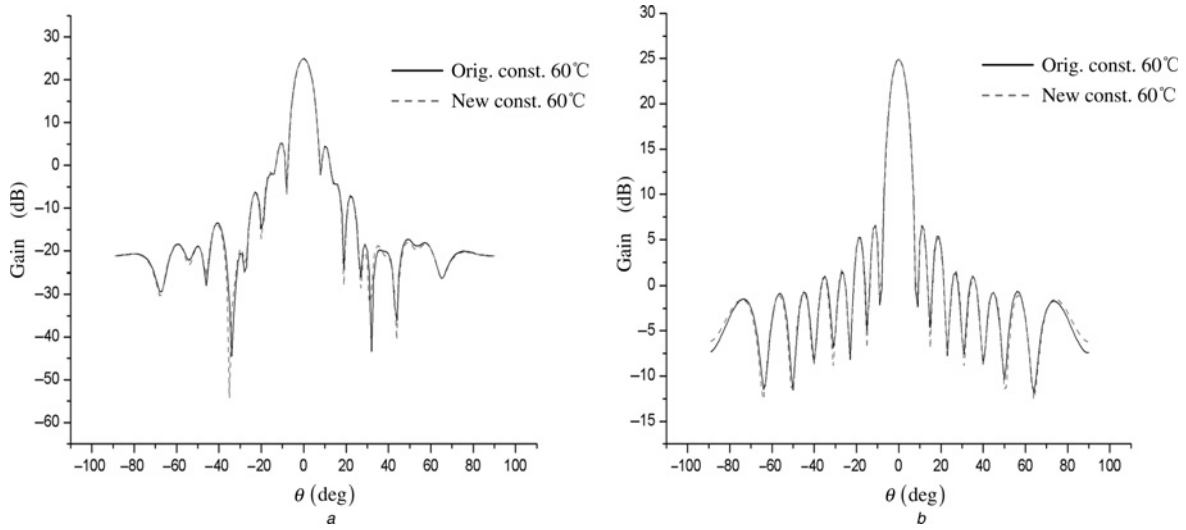

Figure 7 *Antenna gain pattern under third operation condition*
a $\phi = 0^\circ$
b $\phi = 90^\circ$

Table 3 Antenna gain and gain loss under different operation conditions

Operation condition		Gain (dB)	Gain loss (dB)
ideal condition		24.8219	0
first operation condition	heat soak 50°C	24.7301	−0.0918
	heat soak 90°C	24.6915	−0.1304
second operation condition	temperature gradient 40–50°C	24.7447	−0.0772
	temperature gradient 40–70°C	24.7174	−0.1045
third operation condition	original constraint 60°C	24.7297	−0.0922
	new constraint 60°C	24.7207	−0.1012

obvious influence on the antenna gain in the *H*-plane ($\phi = 0^\circ$), with the small influence on the SLL. Furthermore, the same structural distortion has no obvious effect on the antenna gain in the *E*-plane ($\phi = 90^\circ$). But the influence on the beam pointing and SLL is great. It is also found that the degradation of EM performances becomes serious with the increase in structure temperature and temperature gradient. The reason is that the position deviation values of radiating elements determine the degradation of EM performances. A comparison of the simulation results of the three operation conditions indicate that the different distortions of the array plane are induced by the different constraint forms. The influence of the different constraint conditions on EM performances is different. The better constraint condition should be adopted to improve the EM performances.

5 Conclusions

A coupled SET model of APAA is developed with the obtained satisfying simulation results: the influence of different temperatures and different structural distortions (structure constraint condition) on the antenna EM performances is different. The position deviation of radiating elements plays a direct role in the degradation of EM performances. By increasing the structure stiffness, reducing the array temperature and temperature gradient and adopting the appropriate constraint format, the EM performances can be greatly improved. The engineering application of the coupled SET model of APAA may decrease the requirement for the precision of structure and lessen the manufacturing difficulty under the precondition that the EM performances of radar antenna are assured. Its application also offers electrical designers the theoretical guidance to design the structural precision index and temperature distribution of APAA.

6 Acknowledgments

This work is supported by the National Natural Science Foundation of China by No. 50805111, the Natural Science Basic Research Plan in Shaanxi Province of China by No. SJ08E$_2$03 and the National Grand Fundamental Research 973 Program of China.

doi: 10.1049/iet-map.2008.0274

7 References

[1] SO J., KIM J., CHEON C.: 'Modeling and design of a finite dual-polarised notch phased-array antenna'. Proc. IEE Microwaves Antennas and Propagation Conf., December 2006, vol. 153, 1, pp. 43–48

[2] HOMMEL H., FELDLE H.P.: 'Current status of airborne active phased array (AESA) radar systems and future trends'. Proc. IEEE MTT-S Int. Conf. Microwave, June 2005, vol. 3, pp. 1449–1452

[3] LACOMME P., SYST T.A., ELANCOURT F.: 'New trends in airborne phased array radars'. Proc. IEEE Int. Conf. Phased Array Systems and Technology, October 2003, pp. 7–12

[4] ZHANG G.Y.: 'Phased array radar technology' (Publishing House of Electronics Industry, 2006) (in Chinese)

[5] SHU X.R., HE B.F., GAO T.: 'Phased array radar antenna' (National Defence Industry Press, 2007) (in Chinese)

[6] AGRAWAL A.K., MATTIOLI J.A., LANDRY N.R.: 'An active phased array antenna packaging scheme'. Proc. IEEE Int. Conf. Antennas and Propagation, July 1996, pp. 1608–1611

[7] KATAGIAND T., CHIBA I.: 'Review on recent phased array antenna technologies in Japan'. Proc. IEEE Int. Conf. Antennas and Propagation, August 2000, vol. 2, pp. 570–573

[8] LARSEN N.V., BREINBJERG O.: 'Modelling the impact of ground planes on antenna radiation using the method of auxiliary sources', *IET Microw., Antennas Propag.*, 2007, **1**, (2), pp. 472–479

[9] DUFORT E.C.: 'Low sidelobe electronically scanned antenna using identical transmit/receive modules', *IEEE Trans. Antennas Propag.*, 1988, **36**, (3), pp. 349–356

[10] WANG H.S.C.: 'Performance of phased-array antennas with mechanical errors', *IEEE Trans. Aerosp. Electron. Syst.*, 1992, **28**, (2), pp. 535–545

[11] ZAGHLOUL A.I., GUPTA R.K., KOH E.C., KILIC O.: 'Design and performance assessment of active phased arrays for communications satellites'. Proc. IEEE Int. Conf. Phased Array Systems and Technology, May 2000, pp. 197–201

[12] LI J.X., GAO T.: 'Analysis of element failure and tolerance in solid-state active phased array', *Mod. Radar*, 1992, **14**, (6), pp. 36–44 (in Chinese)

[13] JIANG W., GUO Y.C., LIU T.H.: 'Comparison of random phasing methods for reducing beam pointing errors in phased array', *IEEE Trans. Antennas Propag.*, 2003, **51**, (4), pp. 782–787

[14] RUZE J.: 'Pattern degradation of space fed phased arrays'. MIT Lincoln Lab., Proj. Report. SBR-1, 1979

[15] MOLLAH M., KARMAKAR N., JEFFREY S.F.: 'Development of phased array antenna by controlling the filling factor of periodic structure', *J. RF Microw. Comput.-Aided Eng.*, 2007, **17**, (3), pp. 353–359

[16] ADELMAN H.M., PADULA S.L.: 'Integrated thermal–structural–electromagnetic design optimization of large space antenna reflectors', NASA-TM-87713, 1986

[17] LIU J.S., HOLLAWAY L.: 'Integrated structure–electromagnetic optimization of large reflector antenna systems', *Struct. Multidiscip. Optim.*, 1998, **16**, (1), pp. 29–36

[18] JOSHI S.C., PARAMANOV V., SKASSYRSKAYA A., *ET AL.*: 'The complete 3-D coupled RF–thermal–structural–RF analysis procedure for a normal conducting accelerating structure for high intensity hadron linac'. Proc. 21st Int. Linac Conf. (LINAC 2002), Gyeongju, Korea, August 2002, pp. 216–218

[19] YE J.: 'Thermal design of phased array antenna', *Electromech. Eng.*, 2001, **17**, (1), pp. 42–46 (in Chinese)

[20] NAKAGAWA M., MORIKAWA E., KOYAMA Y.: 'Development of thermal control for phased array antenna'. Proc. 21st Int. Communications Satellite Systems Conf., April 2003, AIAA-2003–2226

[21] DUAN B.Y., QI Y.H.: 'Study on optimization of mechanical and electronic synthesis for the antenna structural systems', *Mechatronics*, 1994, **4**, (6), pp. 553–564

[22] ZAGHLOUL A.I., KILIC O., KOHLS E.C.: 'System aspects and impairments of active phased arrays for satellite communications', *IEEE Trans. Aerosp. Electron. Syst.*, 2007, **43**, (1), pp. 176–186

[23] YAJIMA M., KURODA T., MAEDA T., SHIMADA M.: 'Active phased array antenna for WINDS satellite'. Proc. 25th AIAA Int. Communications Satellite Systems Conf., April 2007, AIAA-2007-3240

[24] WANG N., XUE Z.H., YANG S.M.: 'Characters of time domain radiated field of ultra wide band ultra low side lobe phased array antenna', *Acta Electron. Sin.*, 2006, **34**, (9), pp. 1605–1609 (in Chinese)

[25] JIANG Q.Q.: 'Development trend of active phased array radar technology', *Technol. Found. Natl Def.*, 2005, **2**, (4), pp. 9–11 (in Chinese)

[26] SEONG N.S., PARK S.O.: 'A radiator element for active phased array antenna', *Microw. Opt. Technol. Lett.*, 2006, **48**, (12), pp. 2393–2395

[27] BETANCOURT D., BOCIO C.R.: 'A novel methodology to feed phased array antennas', *IEEE Trans. Antennas Propag.*, 2007, **55**, (9), pp. 2489–2494

[28] TONN D.A., BANSAL R.: 'Reduction of sidelobe levels in interrupted phased array antennas by means of a genetic algorithm', *J. RF Microw. Comput.-Aided Eng.*, 2007, **17**, (2), pp. 134–141

8 Appendix A: EM analysis of planar hexagonal APAA

It is supposed that a planar hexagonal APAA locates in the $O-xy$ plane, the interval of the array element is d_x, the interval of the row element is d_y, the base angle of the array is β and the coordinate system is shown in Fig. 8. The distance vector of the element (m, n) to element $(0, 0)$ located in the origin O of the coordinate system is given as

$$\vec{r}_{mn} = m\vec{a}_1 + n\vec{a}_2 \ (m = 0, 1, 2, \ldots, \ n = 0, \ \pm 1, \ \pm 2, \ \ldots) \tag{11}$$

where $\vec{a}_1$ and $\vec{a}_2$ are the unit vectors of the base and hypotenuse of a basic triangle, respectively.

(θ, ϕ) is set as the direction of the target relative to the coordinate system $O-xyz$, whose direction cosine is (cos α_x, cos α_y, cos α_z). According to the space geometry relation illustrated in Fig. 9, the relationship between the angle of the far-field target to the coordinate axial and the direction cosine is given as

$$\cos\alpha_x = \sin\theta\cos\phi, \ \cos\alpha_y = \sin\theta\sin\phi, \ \cos\alpha_z = \cos\theta \tag{12}$$

When the structural distortion of APAA is determined, the displacement of element (i, j) is taken as $(\Delta x_{ij}, \Delta y_{ij}, \Delta z_{ij})$. Then what follows is the space phase difference of two

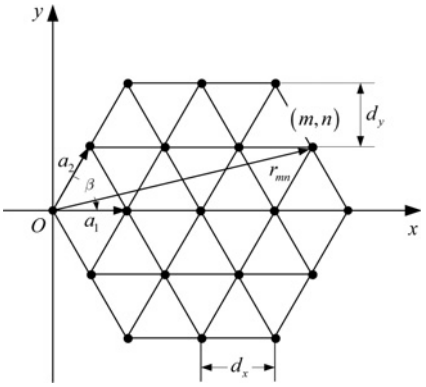

Figure 8 *Element configuration of planar hexagonal APAA*

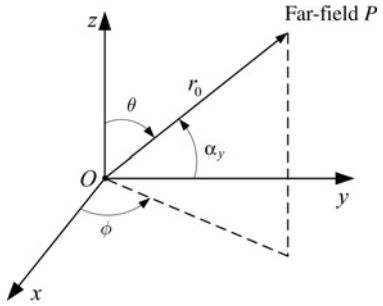

Figure 9 *Space geometrical relationship of far-field target*

adjacent elements in $\vec{a}_1$, $\vec{a}_2$ and z-axis directions, respectively

$$\begin{aligned}\Delta\varphi_1 &= k(d_x + \Delta x_{ij})\cos\alpha_x, \ \Delta\varphi_2 \\ &= k\left[(d_y + \Delta y_{ij})\frac{\cos\beta}{\sin\beta}\cos\phi + (d_y + \Delta y_{ij})\sin\phi\right] \\ &\quad \times \sin\theta, \ \Delta\varphi_z = k\Delta z_{ij}\cos\alpha_z\end{aligned} \tag{13}$$

where $k = 2\pi/\lambda$ and λ is the operation wavelength.

As a result, the phase difference of element (m, n) $(0 \le m \le M-1, \ 0 \le n \le N-1)$ in regard to element $(0, 0)$ is obtained

$$\begin{aligned}\Delta\varphi_{mn} &= \sum_{i=1}^{m}\Delta\varphi_1 + \sum_{j=1}^{n}\Delta\varphi_2 + \Delta\varphi_z + S_{mn} \\ &= k\left(md_x + \sum_{i=0}^{m}\Delta x_{ij}\right)\cos\alpha_x + k\left(nd_y + \sum_{i=0}^{m}\Delta y_{ij}\right) \\ &\quad \times \frac{\cos\beta}{\sin\beta}\cos\phi\sin\theta + k\left(nd_y + \sum_{i=0}^{m}\Delta y_{ij}\right) \\ &\quad \times \sin\phi\sin\theta + k\Delta z_{ij}\cos\alpha_z + S_{mn}\end{aligned} \tag{14}$$

According to the superposition principle of the EM field, the radiation field of APAA is expressed as

$$\begin{aligned}E &= E_{00} + E_{01} + \cdots + E_{mn} + \cdots + E_{M-1,N-1} \\ &= E_{00}(1 + e^{j\varphi_{01}} + \cdots + e^{j\varphi_{mn}} + \cdots + e^{j\varphi_{M-1,N-1}})\end{aligned} \tag{15}$$

If the mutual coupling of the radiating element is not considered, the principle of the pattern multiplication is given based on (15) as follows

Pattern function of array antenna
= Pattern of element
× Function of array factor with different arrangements

doi: 10.1049/iet-map.2008.0274

The mathematical expression of the above principle is also

$$E = E_e \sum_{m=0}^{M-1} \sum_{n=0}^{N-1} I_{mn} \exp(j\varphi_{mn}) \tag{16}$$

where E_e is the pattern function of the radiating element and I_{mn} is the amplitude of excitation current.

According to (12), the substitution of (16) and (14) into (15) yields the pattern function of the planar hexagonal APAA as

$$\begin{aligned} E(\theta, \phi) = \sum_{m=0}^{M-1} \sum_{n=0}^{N-1} E_e I_{mn} \exp\Bigg\{ jk\Bigg[&\left(md_x + \sum_{i=0}^{m} \Delta x_{ij} \right) \\ &\times \sin\theta\cos\phi + \left(nd_y + \sum_{i=0}^{m} \Delta y_{ij} \right) \frac{\cos\beta}{\sin\beta} \sin\theta\cos\phi \\ &+ \left(nd_y + \sum_{i=0}^{m} \Delta y_{ij} \right) \sin\theta\sin\phi \\ &+ \Delta z_{ij}\cos\theta \Bigg] + jS_{mn} \Bigg\} \end{aligned} \tag{17}$$

9 Appendix B: EM analysis of planar rectangular APAA

It is assumed that the radiating elements of a planar rectangular APAA are assembled with an equal interval in between, which is shown in Fig. 10. The number of radiating elements is $M \times N$ in the O–xy plane. The intervals of the radiating elements in the azimuth and elevation directions are d_x and d_y, respectively. The design coordinate of element (i, j) is $(id_x, jd_y, 0)$. When the structural distortion of APAA is determined, the displacement of element (i, j) is taken as $(\Delta x_{ij}, \Delta y_{ij}, \Delta z_{ij})$. Then the coordinate of the distorted radiating element is given as

$$(id_x + \Delta x_{ij}, jd_y + \Delta y_{ij}, \Delta z_{ij})$$

The space phase difference of two adjacent elements of the planar rectangular APAA in the x-, y- and z-axis directions

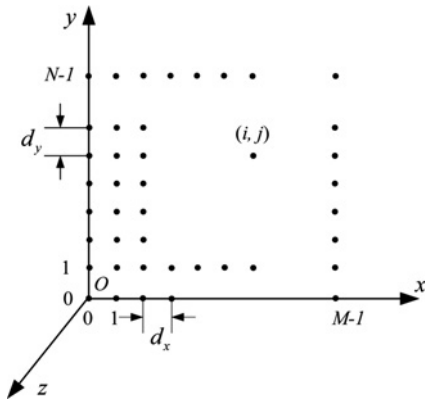

Figure 10 *Element configuration of planar rectangular APAA*

in the far-field target is determined, respectively, as follows

$$\begin{aligned} \Delta\varphi_x &= k(d_x + \Delta x_{ij})\cos\alpha_x,\ \Delta\varphi_y \\ &= k(d_y + \Delta y_{ij})\cos\alpha_y,\ \Delta\varphi_z \\ &= k\Delta z_{ij}\cos\alpha_z \end{aligned} \tag{18}$$

Therefore the phase difference of element (m, n) in regard to element $(0, 0)$ is obtained

$$\begin{aligned} \Delta\varphi_{mn} &= \sum_{i=1}^{m} \Delta\varphi_x + \sum_{j=1}^{n} \Delta\varphi_y + \Delta\varphi_z + S_{mn} \\ &= kmd_x\cos\alpha_x + k\sum_{i=0}^{m} \Delta x_{ij}\cos\alpha_x + knd_y\cos\alpha_y \\ &\quad + k\sum_{j=0}^{n} \Delta y_{ij}\cos\alpha_y + k\Delta z_{ij}\cos\alpha_z + S_{mn} \end{aligned} \tag{19}$$

Similarly, the pattern function of the planar rectangular APAA is derived as follows

$$\begin{aligned} E(\theta, \phi) = \sum_{m=0}^{M-1} \sum_{n=0}^{N-1} E_e I_{mn} \exp\Bigg\{ jk\Bigg[&\left(md_x + \sum_{i=0}^{m} \Delta x_{ij} \right) \sin\theta\cos\phi \\ &+ \left(nd_y + \sum_{j=0}^{n} \Delta y_{ij} \right) \sin\theta\sin\phi + \Delta z_{ij}\cos\theta \Bigg] + jS_{mn} \Bigg\} \end{aligned} \tag{20}$$